

# Phase-locking of a 2.7-THz quantum cascade laser to a mode-locked erbium-doped fibre laser

Stefano Barbieri<sup>1\*</sup>, Pierre Gellie<sup>1</sup>, Giorgio Santarelli<sup>2</sup>, Lu Ding<sup>1</sup>, Wilfried Maineult<sup>1</sup>, Carlo Sirtori<sup>1</sup>, Raffaele Colombelli<sup>3</sup>, Harvey Beere<sup>4</sup> and David Ritchie<sup>4</sup>

**Mode-locked femtosecond lasers have revolutionized the field of optical metrology by allowing the realization of ultra-stable phase-coherent links between the optical-frequency domain and the radiofrequency range<sup>1–4</sup>. In this work we have used the electro-optic effect in ZnTe (ref. 5) to demonstrate that the frequency and the phase of a 2.7 THz quantum cascade laser<sup>6</sup> can be actively stabilized to the  $n$ th harmonic of the 90 MHz repetition rate ( $f_{\text{rep}}$ ) of a commercial, mode-locked erbium-doped fibre laser<sup>7</sup>. The beating between the stabilized quantum cascade laser frequency and the harmonic of  $f_{\text{rep}}$  yield a signal-to-noise ratio of 80 dB in a bandwidth of 1 Hz. The technique is inherently broadband, that is, it is applicable to any quantum cascade laser source provided that its frequency falls within the spectral bandwidth of the femtosecond laser ( $\sim 5$  THz)<sup>8,9</sup>. Furthermore, it is an ideal tool with which to control the phase of different quantum cascade lasers using light and compact fibre technology rather than superconducting bolometer mixers<sup>10,11</sup>.**

Frequency- and phase-stabilized, high-power, solid-state terahertz sources can find applications in a number of different fields, from far-infrared astronomy and high-precision molecular gas spectroscopy<sup>12,13</sup> to telecommunications, providing the carrier wave for broadband wireless links<sup>14,15</sup>. To this extent terahertz quantum cascade lasers (QCLs)<sup>16,17</sup> are promising sources, operating at frequencies between  $\sim 1.2$  and 4.5 THz with power levels in the range of tens of milliwatts and at temperatures in continuous-wave (c.w.) above liquid nitrogen.

Phase-locking of a terahertz QCL to a stable electronic oscillator was recently demonstrated<sup>10</sup>, with a 20-GHz oscillator upconverted to 1.4993 THz using a classical multiplier chain, then mixed with the frequency of a QCL at 1.5005 THz using a superconducting hot-electron bolometer. This work was followed soon after by phase-locking of a 2.7-THz QCL using an analogous technique<sup>11</sup>. In the latter case, 13% of the QCL total power was locked to the reference signal.

Locking techniques such as those briefly described above are bound by the necessity of multiplying the original radiofrequency (RF) oscillator by a factor of  $\sim 100$ –200. The use of such extreme multiplication orders has two main inconveniences: (i) it limits the spectral tuning at the end of the chain to  $\sim 10\%$  of the centre frequency, and (ii) it generates low power levels that restrict the choice of mixer element to superconducting receivers. In this work we use a different approach, based on ref. 7, that allows the phase-locking of any terahertz QCL, regardless of its emission frequency, without the use of multiplier chains, using a room-temperature-operated detector for beat-note detection. Essentially, as we shall show, it takes

advantage of the fact that the spectrum of a mode-locked laser is composed of a comb of evenly spaced lines spanning several terahertz of frequency<sup>18</sup>. The frequency of the  $n$ th line is given by  $\nu_n = n \times f_{\text{rep}} + f_0$ , where  $n$  is an integer,  $f_0$  is the so-called frequency offset<sup>2</sup>, and  $f_{\text{rep}}$  lies typically in the 100 MHz range.

The detection technique used in the experiment is illustrated in Fig. 1. It uses a standard ZnTe crystal, in series with an oriented pair of  $\lambda/4$  and  $\lambda/2$  wave plates, followed by a polarizing beamsplitter (PBS) and a fast balanced-photodiodes assembly<sup>5</sup>. The c.w. terahertz QCL and a frequency-doubled 1,550-nm mode-locked fibre laser are simultaneously focused on the ZnTe crystal. Thanks to the Pockels effect, the combination of ZnTe with the optical elements of Fig. 1 modulates the amplitude of the femtosecond laser beam at the frequency of the terahertz QCL,  $\nu_{\text{QCL}} = 2.7$  THz (see Methods)<sup>19</sup>. As is schematically shown in Fig. 2, and assuming that the QCL emits on a single mode, in the frequency domain this gives rise to two replicas (or modulation sidebands) on each side of the femtosecond laser spectrum at  $\pm \nu_{\text{QCL}}$  from its centre. Because the femtosecond laser bandwidth,  $\Delta_{\text{BW}} \approx 5$  THz  $> \nu_{\text{QCL}}$ , the sidebands overlap with the original carrier. Therefore, as a result of the quadratic detection of the photodiodes, we obtain (see Fig. 2a) a number of low-frequency beat-notes oscillating at  $\delta f_- = (\nu_{\text{QCL}} - n \times f_{\text{rep}})$  and  $\delta f_+ = (n + 1) \times f_{\text{rep}} - \nu_{\text{QCL}} = f_{\text{rep}} - \delta f_-$ . Here,  $f_{\text{rep}} = 90$  MHz and  $n \times f_{\text{rep}}$  is the closest harmonic to  $\nu_{\text{QCL}}$ . Note that in the beat-note generation the frequency offset  $f_0$  is subtracted, and  $\delta f_-$ ,  $\delta f_+$  depend only on  $\nu_{\text{QCL}}$  and  $f_{\text{rep}}$  (refs. 8,9). A direct terahertz  $\rightarrow$  megahertz link is therefore obtained, from 2.7 THz down to  $f_{\text{rep}} = 90$  MHz. An important parameter that can influence the efficiency of the detection process is phase-matching between the terahertz and the femtosecond beam. Indeed, as well as having a large electro-optic coefficient, the choice of ZnTe was dictated by the fact that at  $\sim 775$  nm (the centre

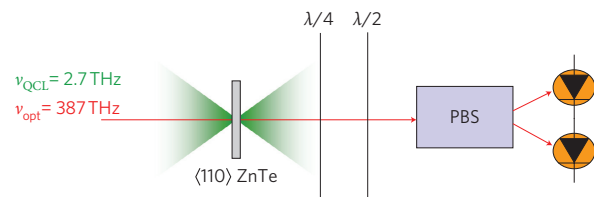


**Figure 1 | Schematic of the electro-optic detection set-up.** Shown from left to right are the ZnTe crystal, the  $\lambda/4$  and  $\lambda/2$  wave plates, the polarizing beamsplitter (PBS) and the two photodiodes. The QCL beam (green) was focused on the ZnTe crystal with an  $f/1$ , gold-coated parabolic mirror. The red line represents the frequency-doubled femtosecond laser beam at  $\sim 387$  THz ( $\sim 775$  nm).

<sup>1</sup>Laboratoire Matériaux et Phénomènes Quantiques, Université Paris 7 and CNRS UMR 7162, 10 rue A. Domont et L. Duquet, 75205 Paris, France,

<sup>2</sup>LNE-SYRTE, CNRS, UPMC, Observatoire de Paris, 61 avenue de l'Observatoire, 75014 Paris, France, <sup>3</sup>Institut d'Electronique Fondamentale, Université Paris Sud and CNRS, UMR 8622, 91405 Orsay, France, <sup>4</sup>Cavendish Laboratory, J. J. Thomson Avenue, Cambridge CB3 0HE, United Kingdom.

\*e-mail: stefano.barbieri@univ-paris-diderot.fr

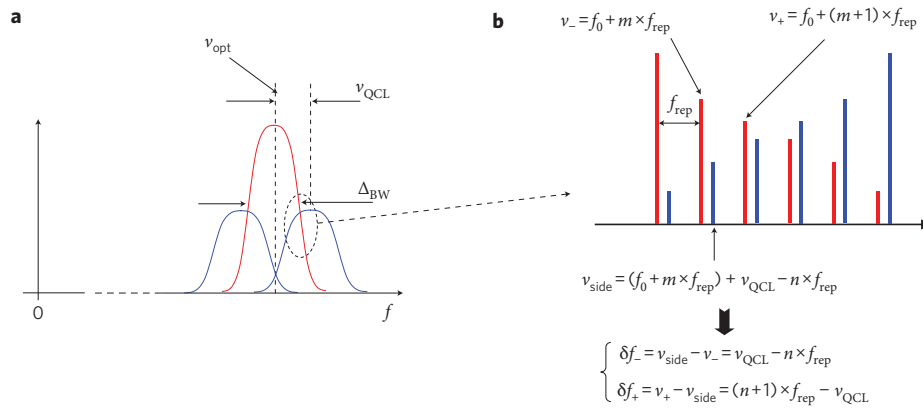


**Figure 2 | Principle of the detection technique.** **a**, Schematic of the spectral envelope of the amplitude-modulated optical beams at the output of the PBS. Red and blue curves represent the optical carrier and the sidebands, respectively, at  $\pm v_{\text{QCL}}$ . **b**, Enlargement of the left panel showing the individual comb teeth of the optical carrier and of the upper terahertz sideband. Here,  $v_-$  and  $v_+$  are the optical carrier comb teeth that lie closest to the generic comb tooth from the upper sideband, labelled  $v_{\text{side}}$ , and  $m$  and  $n$  are integer numbers.  $\delta f_-$  is the low-frequency beat-note signal used for phase-locking (see text).

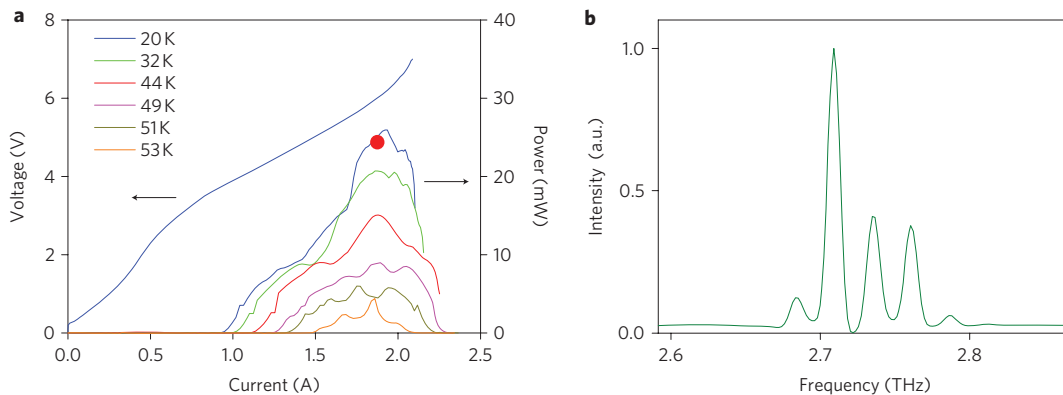


**Figure 3 | QCL electrical and optical characteristics.** **a**, Plot showing c.w. optical power versus current characteristics of the QCL used in this work at different temperatures. A voltage versus current characteristic at 20 K is also displayed. **b**, Representative terahertz emission spectrum measured at 20 K and for a current of 1.76 A (red dot in **a**).

wavelength of our femtosecond laser beam) phase-matching occurs at  $\sim 2.4$  THz, yielding a coherence length of a few millimetres at least up to 3 THz (ref. 20).

The QCL used in this work is based on a 12- $\mu\text{m}$ -thick  $\text{Al}_{0.15}\text{Ga}_{0.85}\text{As}$ -GaAs active region grown by molecular beam epitaxy<sup>6</sup>. Devices were fabricated into 3-mm-long single-plasmon waveguides that were indium-soldered to copper holders. These were screwed on the cold-head of a helium cryostat. In Fig. 3a we report the c.w. optical and electrical characteristics at different temperatures of the device used in this work. The maximum output power is 27 mW. Figure 3b shows an emission spectrum measured at 20 K, at a current of 1.76 A. It is composed of five longitudinal Fabry-Perot (FP) modes separated by the cavity roundtrip frequency of approximately 13 GHz. The linewidth of each mode is limited by the resolution of the Fourier transform infrared (FTIR) spectrometer ( $0.25\text{ cm}^{-1}$ ; 7.5 GHz).

The experimental set-up for the phase-locking is shown in Fig. 4. The terahertz QCL radiation was collected and focused on a 1-mm-thick  $\langle 110 \rangle$  ZnTe crystal with the help of two parabolic mirrors. The beam from a  $\sim 150$ -fs mode-locked erbium-fibre laser (Toptica FFS) was first frequency-doubled using a  $\beta$ -barium borate (BBO) crystal and then collinearly superimposed on the terahertz focus (see the measured optical spectrum in Fig. 4b). After the PBS, two optical beams of 6 mW average power were focused on a balanced detection unit (see Methods for details), and the photocurrent spectrum monitored with a microwave spectrum analyser. In Fig. 4c we report an

example of a fast RF spectrum recorded in the 0–93 MHz interval with a sweep time of 13 ms and a resolution bandwidth (RBW) of 100 kHz. Here, the QCL is driven in current mode with 1.766 A, and its temperature is stabilized to  $20 \pm 0.01$  K. Two groups of three peaks are clearly visible, symmetrically positioned with respect to  $f_{\text{rep}}/2$  ( $= 44.6$  MHz). From the terahertz QCL spectrum of Fig. 3b, these can be identified as the beat-notes at  $\delta f_{\pm}$  and  $\delta f_{\pm} = f_{\text{rep}} - \delta f_{\pm}$ , from each of the three main longitudinal FP modes of the QCL (see Fig. 2b). The relative position between the peaks is obviously not preserved because the terahertz mode spacing ( $\sim 13$  GHz) is much larger than 90 MHz, and each mode is beating with its closest harmonics of  $f_{\text{rep}}$ . From each individual beat-note we measured a free-running linewidth and a current-tuning similar to those found in the literature using a number of techniques (see Methods for a discussion of the effect of optical feedback)<sup>21–23</sup>. For phase-locking of the QCL, a band-pass filter with a bandwidth of 10 MHz and centred at 30 MHz was used to reduce the magnitude of the lower-intensity spurious beat-note signals with respect to the main signal. (The frequency of the main beat-note signal could be moved from the 38 MHz of Fig. 4c by fine tuning of the temperature and current; see Methods.) This step, which could have been avoided if our QCL was single-mode<sup>24</sup>, is crucial to obtain a sufficiently clean beat-note signal (see Methods). After filtering, the main beat-note signal (see  $\delta f_-$  in Fig. 2b) was amplified and compared using a RF mixer to a reference signal of frequency  $f_{\text{RF}} \approx 30$  MHz, generated

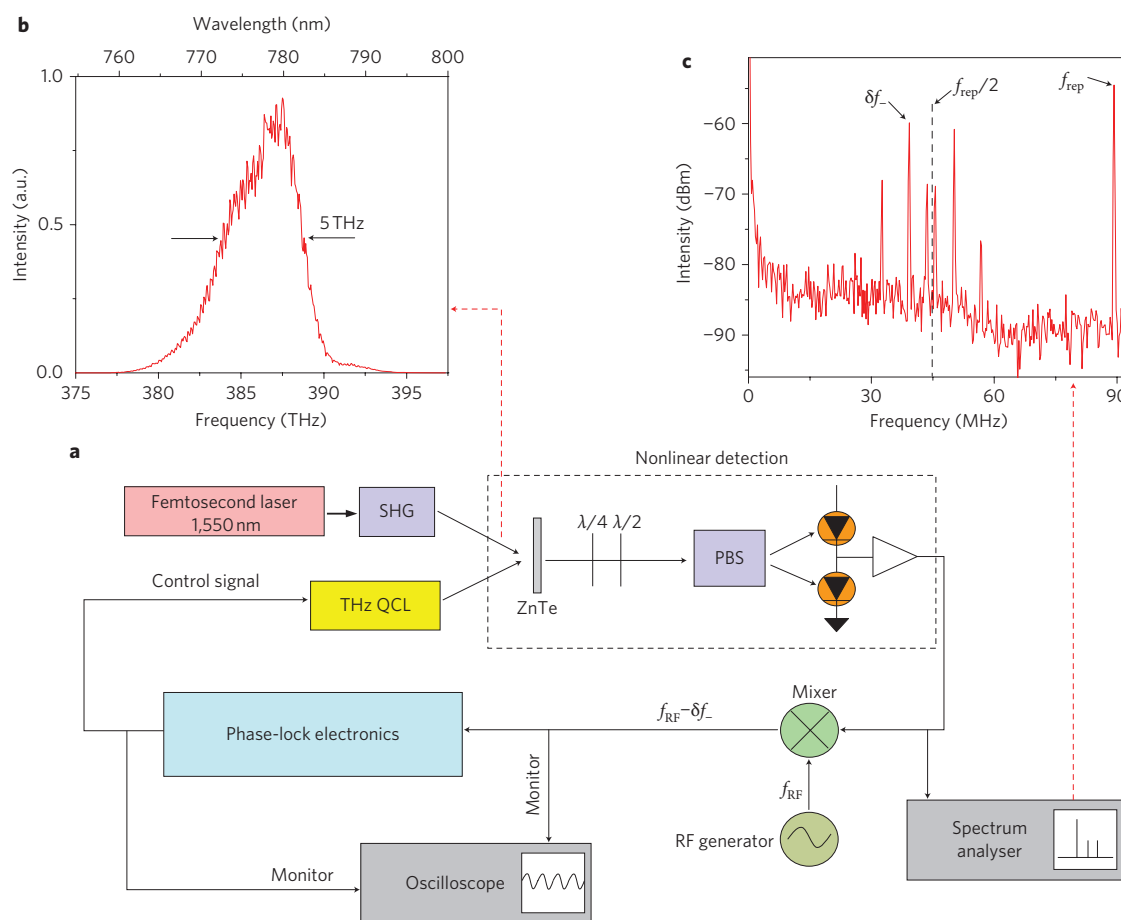


**Figure 4 | Experimental set-up.** **a**, Schematic of the experimental set-up. **b**, Spectrum of the femtosecond laser measured with an optical spectrum analyser after the second harmonic generation (SHG) stage. **c**, Unlocked RF spectrum of the beat-note signal. The spectrum was collected in the 0–90 MHz range with a sweep time of 13 ms and a RBW of 100 kHz. The roll-off at  $\sim 50$  MHz is due to the low-pass filter in series with the balanced detection unit.  $\delta f_- \approx 38$  MHz is produced by the most intense longitudinal mode of the QCL (see Fig. 3b), and was used for stabilization.

by a frequency synthesizer. The error signal, oscillating at  $f_{\text{error}} = f_{\text{RF}} - \delta f_-$ , was fed into fast phase-lock electronics and used to control a small fraction of the terahertz QCL bias current. In Fig. 5 we report the RF spectra of the unlocked (Fig. 5a) and locked (Fig. 5b–d) beat-note signal with RBW decreasing from 1 MHz to 1 Hz, the spectral resolution limit of our spectrum analyser. From Fig. 5b we find that the control bandwidth of the phase-lock is  $\sim 1.5$  MHz, not limited by the electronic circuit. For all the spectra the maximum intensity of the beat-note remains fixed at  $-25$  dBm, and the noise floor scales with the RBW, from  $-45$  dBm with 1-MHz RBW, to  $-104$  dBm with 1-Hz RBW (with 100 video bandwidth averages). From Fig. 5b we estimate that nearly 90% of the QCL longitudinal mode power is phase-locked to the  $n$ th harmonic of  $f_{\text{rep}}$ . (see Methods for the derivation)<sup>25,26</sup>.

In conclusion, we have achieved phase-locking of a longitudinal mode of a 2.7-THz QCL, yielding an RF beat-note signal with 80 dB of signal-to-noise ratio and a bandwidth of 1 Hz. The technique takes advantage of the linear electro-optic effect to amplitude-modulate a mode-locked femtosecond fibre laser. From the point of view of applications we believe that our demonstration opens up new perspectives for the use of terahertz QCLs not just as stabilized local oscillator sources. Indeed, there are two other advantages in using a femtosecond laser for phase-locking, namely (i) phase-locking two or more QCLs simultaneously using the same femtosecond laser and (ii) transporting the femtosecond laser signal with an optical fibre. These possibilities could be used to achieve terahertz electronic beam-steering with a terahertz QCL phased array,

or for remote imaging/sensing based on the detection scheme of ref. 7. Finally, note that in this work we used the Pockels effect in a ZnTe crystal; however, the use of other types of crystals, such as GaAs or 4-dimethylamino-*N*-methyl-4-stilbazolium-tosylate (DAST), or a nonlinear terahertz  $\rightarrow$  near-IR upconversion technique that we have demonstrated, could allow a phase-lock directly at 1.5  $\mu\text{m}$ , without the frequency-doubling stage<sup>20,27–29</sup>. The use of semiconductor photomixers is also an option<sup>18,29</sup>.

## Methods

**Detection technique.** In the detection scheme of Fig. 1, the terahertz QCL and the femtosecond laser beams are linearly polarized and oriented at  $45^\circ$  with respect to the  $\langle 1, -1, 0 \rangle$  direction of the ZnTe crystal. The  $\lambda/4$  wave plate compensates the residual birefringence of the ZnTe crystal (see ref. 19 for details). In this way, in the absence of terahertz radiation, the polarization of the femtosecond laser after the ZnTe is converted from elliptical to linear polarization. Finally the  $\lambda/2$  wave plate orients the linear polarization at  $45^\circ$  with respect to the axes of the PBS. In the approximation of small rotation angles one can show that the amplitude of each optical beam at the output of the PBS is proportional to  $E_{\text{THz}}(t) \times E_{\text{opt}}(t)$ , where  $E_{\text{THz}}$  and  $E_{\text{opt}}$  are the electric fields of the terahertz and femtosecond beams, respectively. The combination ZnTe +  $\lambda/4$  +  $\lambda/2$  acts as an electro-optic amplitude modulator driven by the terahertz a.c. field.

**Balanced detection unit.** The balanced detection unit is composed of two wide-area silicon photodiodes (Hamamatsu S3399) and a trans-impedance amplifier. The system bandwidth is  $\sim 300$  MHz. The femtosecond laser comb has a wide-band excess amplitude noise  $\sim 10$ – $15$  dB above the shot noise. The balanced detection efficiently suppresses this excess noise from close to d.c. to  $f_{\text{rep}}/2$ .

**Linewidth and effect of optical feedback.** We found that the separation between the RF peaks due to different FP modes could be moved by several tens of megahertz by

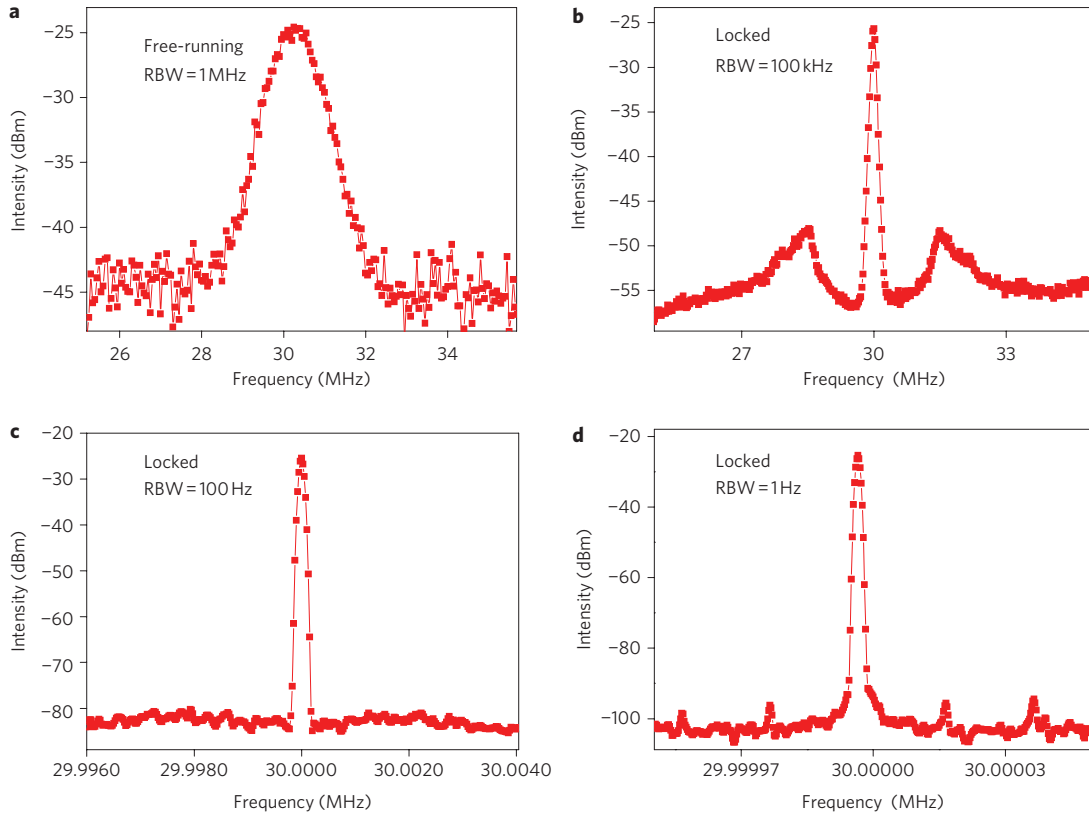


**Figure 5 | RF spectra.** **a–d**, Unlocked (**a**) and locked (**b–d**) RF spectra of the beat-note signals with RBW decreasing from 1 MHz to 1 Hz, the spectral resolution limit of our spectrum analyser. Spectra were collected with 100 video bandwidth averages. The two sidebands of **b** indicate that the bandwidth of the phase-lock is  $\sim 1.5$  MHz.

changing the distance between the QCL and the ZnTe crystal or by moving the QCL in the focal plane. Similar effects have already been reported in ref. 21, and are the result of a frequency pulling produced by an optical feedback effect that it is not possible to avoid using simple methods such as tilting the QCL and defocusing or attenuating the terahertz beam. We cannot rule out the free-running linewidth of the laser being affected by such feedback. On the other hand, we measured a RBW-limited linewidth of  $\sim 1$  MHz with a sweep time of 4 ms (see Fig. 5a), and a current tuning of approximately  $3 \text{ MHz mA}^{-1}$ . These values agree with those found in the literature<sup>21–23</sup>. It is worth noting that these spectral characteristics are inherent to the QCL only. Indeed, in the near-IR domain, a fibre-based femtosecond comb tooth has a typical linewidth of  $\sim 100$  kHz, with a frequency drift below 1 MHz over a timescale of a few seconds. However, owing to the inherent optical-to-terahertz frequency division process, the equivalent comb linewidth at  $n \times f_{\text{rep}} \approx 2.7 \text{ THz}$  is  $\sim 1$  kHz, with a frequency drift in the  $\text{kHz s}^{-1}$  range.

**Effect of additional longitudinal modes on the phase-lock.** For the phase-lock of the main QCL longitudinal mode ( $\delta f_{-}$  in Fig. 4c) we experimentally verified that having the beat-note signals generated by the additional longitudinal FP modes (i) sufficiently far apart and (ii) with a low intensity, were crucial requirements in allowing phase-locking. As a rule of thumb, we found that the frequencies of these lines should be at a distance from  $\delta f_{-}$  larger than the phase-lock bandwidth ( $\sim 1.5$  MHz, see Fig. 5b) and with an intensity at least 20 dB below the line to be locked. We obtained these conditions by slightly changing the temperature and current of the QCL, which resulted in fine-tuning of the positions of the peaks. In particular, the frequency of the main beat-note signal was moved from the 38 MHz of Fig. 4c to 30 MHz, and was subsequently filtered using a 10-MHz wide band-pass filter.

**Phase-locked power.** To estimate the fraction of terahertz power in the locked peak of Fig. 5 we used the method described in ref. 25. By numerically integrating the normalized beat-note spectrum of Fig. 5b from 1 Hz to 1.5 MHz (that is, the phase-lock bandwidth) from the centre frequency, and by rescaling by the RBW (100 kHz), we found that  $\sim 90\%$  of the QCL power is effectively phase-locked.

From Fig. 3b we note that  $\sim 15$  mW of power is concentrated in the main longitudinal mode of the QCL, yielding a  $\sim 20$ -dB signal-to-noise ratio in a 1-MHz RBW when the QCL is free-running (Fig. 5a). Considering that (i) the signal on the spectrum analyser is proportional to  $(\delta I_{\text{ph}})^2 \approx (E_{\text{THz}} \times |E_{\text{opt}}|^2)^2 = P_{\text{THz}} \times (P_{\text{opt}})^2$  and (ii) the shot-noise limit is proportional to  $P_{\text{opt}}$ , we obtain a signal-to-noise ratio

in a given RBW that scales linearly with both the QCL power ( $P_{\text{THz}}$ ) and the optical power ( $P_{\text{opt}}$ ). This means that by increasing the optical power by a factor of 3 to  $\sim 20$  mW per photodiode, a QCL power of 1 mW would give a signal-to-noise ratio of  $\sim 13$  dB in the lock bandwidth, which is still sufficient to perform the phase-lock with an acceptable cycle slip rate ( $\sim 0.1 \text{ s}^{-1}$ ) (ref. 26).

Received 24 December 2009; accepted 20 April 2010;  
published online 20 June 2010

## References

- Udem, Th., Holzwarth, R. & Hansch, T. W. Optical frequency metrology. *Nature* **416**, 233–237 (2002).
- Jones, D. J. *et al.* Carrier-envelope phase control of femtosecond mode-locked lasers and direct optical frequency synthesis. *Science* **288**, 635–699 (2000).
- Reichert, J. *et al.* Phase coherent vacuum-ultraviolet to radio frequency comparison with a mode-locked laser. *Phys. Rev. Lett.* **84**, 3232–3235 (2000).
- Maddaloni, P., Cancio, P. & De Natale, P. Optical comb generators for laser frequency measurement. *Meas. Sci. Technol.* **20**, 1–19 (2009).
- Sakai, K. (Ed.) *Terahertz Optoelectronics* (Springer, 2005).
- Barbieri, S. *et al.* 2.9 THz quantum cascade lasers operating up to 70 K in continuous wave. *Appl. Phys. Lett.* **85**, 1674–1676 (2004).
- Löffler, T. *et al.* Continuous wave THz imaging with a hybrid system. *Appl. Phys. Lett.* **90**, 091111 (2007).
- Amy-Klein, A. *et al.* Absolute frequency measurement in the 28-THz spectral region with a femtosecond laser comb and a long-distance optical link to a primary standard. *Appl. Phys. B* **78**, 25–27 (2004).
- Amy-Klein, A. *et al.* Absolute frequency measurement of a SF6 two-photon line by use of a femtosecond optical comb and sum-frequency generation. *Opt. Lett.* **30**, 3320–3322 (2005).
- Rabanus, D. *et al.* Phase locking of a 1.5 THz quantum cascade laser and use as a local oscillator in a heterodyne HEB receiver. *Opt. Express* **17**, 1159–1168 (2009).
- Khosropanah, P. *et al.* Phase locking of a 2.7 THz quantum cascade laser to a microwave reference. *Opt. Lett.* **34**, 2958–2960 (2009).
- Mittleman, D. M. *Sensing with THz Radiation* (Springer, 2003).
- Reix, J.-M. *et al.* The Herschel/Planck programme, technical challenges for two science missions, successfully launched. *Acta Astronomica* **34**, 130–148 (2009).
- Tonouchi, M. Cutting edge terahertz technology. *Nature Photon.* **1**, 97–105 (2007).

15. Capasso, F. *et al.* Quantum cascade lasers: ultrahigh-speed operation, optical wireless communication, narrow linewidth and far-infrared emission. *IEEE J. Quantum Electron.* **38**, 511–532 (2002).
16. Köhler, R. *et al.* Terahertz semiconductor-heterostructure laser. *Nature* **417**, 156–159 (2002).
17. Williams, B. S. Terahertz quantum cascade lasers. *Nature Photon.* **1**, 517–525 (2007).
18. Yasui, T. *et al.* Real-time monitoring of continuous-wave terahertz radiation using a fiber-based, terahertz-comb-referenced spectrum analyzer. *Opt. Express* **17**, 17034–17043 (2009).
19. Duvillaret, L., Raillant, S. & Coutaz, J.-L. Electro-optic sensors for electric field measurements. I. Theoretical comparison among different modulation techniques. *J. Opt. Soc. Am. B* **19**, 2692–2702 (2002).
20. Nahata, A., Weling, A. S. & Heinz, T. F. A wideband coherent terahertz spectroscopy system using optical rectification and electro-optic sampling. *Appl. Phys. Lett.* **69**, 2321–2323 (1996).
21. Barbieri, S. *et al.* Heterodyne mixing of two far-infrared quantum cascade lasers by use of a point-contact Schottky diode. *Opt. Lett.* **29**, 1632–1634 (2004).
22. Barkan, A. *et al.* Linewidth and tuning characteristics of terahertz quantum cascade lasers. *Opt. Lett.* **29**, 575–577 (2004).
23. Hensley, J. M. *et al.* Spectral behaviour of a terahertz quantum cascade laser. *Opt. Express* **17**, 20476–20483 (2009).
24. Demichel, O. *et al.* Surface plasmon photonic structures in terahertz quantum cascade lasers. *Opt. Express* **14**, 5335–5345 (2006).
25. Santarelli, G. *et al.* Heterodyne optical phase-locking of extended-cavity semiconductor lasers at 9 GHz. *Opt. Commun.* **104**, 339–344 (1994).
26. Blanchard, A. *Phase-Locked Loops*, Ch. 12 (Wiley, 1976).
27. Suizu, K., Miyamoto, K., Yamashita, T. & Ito, H. High-power terahertz-wave generation using DAST crystal and detection using mid-infrared powermeter. *Opt. Lett.* **32**, 2885–2887 (2007).
28. Dhillon, S. *et al.* Terahertz transfer onto a telecom optical carrier. *Nature Photon.* **1**, 411–415 (2007).
29. Yokoyama, S., Nakamura, R., Nose, M., Araki, T. & Yasui, T. Terahertz spectrum analyzer based on a terahertz frequency comb. *Opt. Express* **16**, 13052–13061 (2008).

### Acknowledgements

The authors thank M. Amato for technical assistance and acknowledge partial financial support from the Délégation Générale pour l'Armement (contract no. 06.34.020) and the initiative C-Nano Ile-de-France (contract TeraCascade). Device fabrication was carried out at the CTU-IEF-Minerve, which was partially funded by the Conseil Général de l'Essonne.

### Author contributions

S.B. conceived and performed the experiment, analysed the data and wrote the paper. P.G. performed the experiment and fabricated the QCL. G.S. conceived and performed the experiment, analysed the data and contributed to the manuscript preparation. L.D. and W.M. contributed to the experimental set-up. C.S. gave conceptual advice, and contributed to data analysis and to the manuscript preparation. R.C. contributed to fabrication of the QCL and to manuscript preparation. H.E.B. and D.A.R. carried out growth of the QCL.

### Additional information

The authors declare no competing financial interests. Reprints and permission information is available online at <http://npg.nature.com/reprintsandpermissions/>. Correspondence and requests for materials should be addressed to S.B.